Received: 8 September 2023 | Accepted: 13 November 2023

DOI: 10.1111/eci.14132

ORIGINAL ARTICLE

WILEY

Lipidomics of triglyceride-rich lipoproteins derived from hyperlipidemic patients on inflammation

Juan Moreno-Vedia[1] | **Dídac Llop**[1,2] | **Ricardo Rodríguez-Calvo**[1,2] | **Núria Plana**[1,2] | **Núria Amigó**[2,3] | **Roser Rosales**[1,2] | **Yaiza Esteban**[1,2] | **Lluís Masana**[1,2] | **Daiana Ibarretxe**[1,2] | **Josefa Girona**[1,2]

[1]Vascular Medicine and Metabolism Unit, Research Unit on Lipids and Atherosclerosis, Sant Joan University Hospital, Universitat Rovira i Virgili. Institut Investigacio Sanitaria Pere Virgili (IISPV), Reus, Spain

[2]Spanish Biomedical Research Centre in Diabetes and Associated Metabolic Disorders (CIBERDEM), Madrid, Spain

[3]Biosfer Teslab SL, Department of Basic Medical Sciences, Universitat Rovira i Virgili (URV), Institut d'Investigació Sanitària Pere Virgili (IISPV), Reus, Spain

Correspondence
Daiana Ibarretxe, Vascular Medicine and Metabolism Unit, Research Unit on Lipids and Atherosclerosis, Sant Joan University Hospital, Universitat Rovira i Virgili. Institut Investigació Sanitaria Pere Virgili (IISPV), Reus, Spain.
Email: daiana.ibarretxe@urv.cat

Funding information
Spanish Biomedical Research Centre in Diabetes and Associated Metabolic Disorders (CIBERDEM); Instituto de Salud Carlos III, Grant/Award Number: PI18/00515

Abstract

Background and aim: Triglyceride-rich lipoproteins (TRLs) can have an important role in atherosclerosis development due to their size and ability to penetrate the endothelium. While high plasma triglyceride (TG) levels and chronic inflammation are relevant in metabolic diseases, it remains unclear whether TGs are atherogenic or which TRL-TG-derived metabolites are responsible for inflammation. Here, we aimed to study the lipidome modifications of TRL particles enriched in TG in patients with hyperlipidemia and their associations with a proinflammatory status both in vivo and in vitro.

Methods: Using proton nuclear magnetic resonance (^{1}H-NMR), we analysed the plasma levels of glycoprotein acetyls and the TRL lipidomic profile of 307 patients with dyslipidemia. THP-1-derived macrophages were used as an in vitro model to explore the molecular inflammatory effects mediated by TRL.

Results: In vivo, higher TRL-TG levels were associated with higher circulating levels of NMR-measured glycoproteins (Glyc-A, Glyc-B and Glyc-F; $p < .001$). Lipidomic analysis showed that TRL-TG enrichment led to decreased cholesterol and phospholipid content ($p < .01$), an increase in omega-9, and a decrease in saturated fatty acids ($p < .001$). THP-1 macrophages exposed to increasing TRL particle concentrations augmented the secretion of IL-1β and TNF-α, which varied based on particle composition. Particles with higher cholesterol and phospholipid contents exerted higher cytokine secretion. The activation of MAPK, Akt/NFκB, and caspase-1 was concurrent with this proinflammatory response.

Conclusions: High TRL-TG levels are associated with a higher systemic inflammatory status and increased particle concentrations. In vitro, higher particle numbers increase proinflammatory cytokine secretion, with cholesterol and phospholipid-rich TRL being more proinflammatory.

KEYWORDS

^{1}H-NMR, atherosclerosis, inflammation, macrophages, triglyceride-rich lipoproteins

1 | INTRODUCTION

Evidence from epidemiological, genetic, pathology and clinical intervention studies has shown that low-density lipoproteins (LDLs) are causal in atherogenesis, a chronic inflammatory disease that triggers most cardiovascular events.[1,2] However, despite the efficacy of LDL-lowering therapies, residual cardiovascular risk remains, which can be partly associated to high triglyceride (TG) levels.[3] Plasma TG concentration is a biomarker of a family of lipoproteins, the triglyceride-rich lipoproteins (TRLs). The TRLs are a spectrum of heterogeneous particles that comprise chylomicrons (present postprandially or in pathological conditions), VLDL and their remnants (including intermediate-density lipoproteins or IDLs). Chylomicrons and VLDL (TRLs) are assembled in the small intestine and in the liver, respectively. Their rate of generation, the efficiency with which TG content is removed by lipolysis, and hepatic clearance will affect plasma levels of TRL.[4] Predisposing genetic factors as well as modifiable risk factors, such as insulin resistance and changes to unhealthy high-carbohydrate diets (among others), may promote obesity and detrimental metabolic effects, characterised in part by an elevation in TRLs.[5] These events contribute to an overproduction and/or a decline in their catabolism that causes the accumulation of TRLs.

Increased numbers of these particles can have an important role in the development and progression of atherosclerosis. This can be attributed to their size (<70 nm). This group of lipoproteins can penetrate the artery wall across the endothelium and be retained in the subendothelial layer.[2,6] The biochemical composition of these lipoproteins is critical for arterial retention and subsequent events, since larger TRL particles can contain up to four times higher cholesterol content per particle than LDL particles, even though TGs are their main component.[7] Additionally, the enriched presence of apolipoprotein (Apo) C-III and Apo E in TRLs is implicated in their binding and retention.[8,9] Recent genetic research supports the causality of TRLs in cardiovascular risk, implicating various genes related to lipoprotein lipase (LPL) function, a key enzyme in TG hydrolysis and clearance that thus regulates plasma TG concentrations, such as *APOA5, APOC3, ANGPTL3, ANGPTL4* and *LPL* itself.[10] Additional studies have shown that increases in TG levels are accompanied by increased levels of C-reactive protein (CRP, a marker of low-grade inflammation), an effect possibly attributed to some of the TRL components.[11]

The described events that favour TRL uptake induce macrophage foam cell formation without the need for structural modifications of the lipoproteins.[2] Particle in situ degradation during lipolysis in the artery wall releases free fatty acids and bioactive lipids that lead to endothelial dysfunction and inflammation. In obese adipose tissue, TG-laden macrophages stimulate the release of proinflammatory cytokines via the polarisation of macrophages to the classically activated M1 phenotype, which can aggravate the inflammatory status of atherosclerotic lesions.[12] Whether TG can directly exert atherogenic effects or which specific TRL-triglyceride (TRL-TG) lipolysis-derived products are implicated in inflammation is a matter of current research. In addition, LPL and TRL lipolysis anti-inflammatory products exist, suggesting a complex balance of pro- and anti-inflammatory effects mediated by TRL lipolysis.[13]

Proton nuclear magnetic resonance (^{1}H-NMR) is a useful tool to detect inflammatory patterns since it can detect acetyl groups linked to plasma acute-phase glycoproteins (Glyc-A and Glyc-B). We and others have recently reported these glycans as stable biomarkers of chronic inflammation.[14–16] Additionally, ^{1}H-NMR can be used for the detection and quantification of different lipid families and species, such as those contained within the TRL fraction. Therefore, NMR technology may be used to investigate specific lipidomic signatures or profiles linked to the molecular processes that TRLs modulate during atherogenic inflammation.

In the present study, we aimed to investigate whether increasing the TG content within the TRL fraction of patients with hyperlipidemia and subsequent changes in the lipidome of these lipoproteins were associated with a proinflammatory status both in vivo and in vitro. To test this hypothesis, ^{1}H-NMR was used to study the metabolomic profile of 307 individuals and for the lipidomic analysis of the TRL fraction of the participants, which was further used to investigate the inflammatory effects mediated by this fraction in macrophages.

2 | MATERIALS AND METHODS

2.1 | Study population and study design

We conducted a cross-sectional study including 307 individuals willing to participate. Participants were attending the Lipid Unit of the Sant Joan de Reus University Hospital due to lipid metabolism disturbances and associated disorders, such as obesity, type 2 diabetes (T2DM) and metabolic syndrome (Met-S). Based on medical guidelines, we identified obesity as a body mass index (BMI) of 30 kg/m2 or greater, T2D as fasting plasma glucose levels ≥126 mg/dL, or glycated haemoglobin (HbA1c) levels ≥6.5%, or the use of hypoglycaemic medication. Hypertension was defined as a systolic blood pressure ≥140 mm Hg, or a

diastolic blood pressure ≥90 mm, or under antihypertensive drugs. Additionally, we recognised Met-S based on the criteria from the Adult Treatment Panel III (ATPIII). Subjects with chronic lung, renal, or cancer diseases were excluded. Patients taking lipid-lowering medications were subjected to a 6-week wash-out period (8 weeks if they were on fibrates).

The Ethical and Clinical Investigation Committee of the Pere Virgili Institute for Health Research (IISPV) authorised this study, which adhered to standards of the Helsinki Declaration. All participants signed a written consent form.

2.2 | Clinical and standard biochemical determinations

Data on physical examination, complete anamnesis and anthropometric data were recorded. Body mass index (BMI) was calculated from the weight and height measurements (kg/m^2). Using a MyLab 60-X Vision sonographer (Esaote), the carotid intima-media thickness (cIMT) of the right and left common carotid arteries was measured in all participants. The mean cIMT was calculated by averaging the readings of both carotid arteries. Plaques were classified as an IMT of more than 1.5 mm or protrusions into the lumen that were 50% thicker than the surrounding IMT. Fasting blood samples were taken from each participant. Prior to usage, aliquots were prepared for rapid storage at −80°C in our center's BioBank. Biochemical parameters, including lipids, apolipoproteins (apoAI, apoB100 and apoCIII), and hsCRP, were assessed using colorimetric, enzymatic and immunoturbidimetric assays (Spinreact; Horiba), which were adapted to the Cobas Mira Plus Autoanalyser (Roche Diagnostics).

2.3 | TRL isolation and pools of TRL-TG

TRL from each individual was obtained from plasma samples by sequential preparative ultracentrifugation, as described by Havel et al.,[17] The TRL fraction, containing VLDL and IDL ($d < 1.019$ g/mL), was obtained in a Kontron rotor at 45.6 in an Optima XPN-100 ultracentrifuge (Beckman Coulter). After the biochemical determination of the triglyceride concentration in the isolated TRL fractions, samples were divided into four quartiles according to their TG content. One hundred and forty-four representative samples from each quartile were pooled for in vitro experiments. Sample pools were placed in semipermeable dialysis membranes (MW: 12–14,000 Da; Medicell) and subjected to a two-step dialysis of 1 h rotating in PBS pH 7.4 at 4°C.

2.4 | Lipoprotein, glycoprotein and TRL lipidomic analysis by ^{1}H-NMR

The Liposcale test®, a new generation 2D-^{1}H-NMR test developed in collaboration with our group,[18] was used to quantify the TRL particle number concentrations (P) and size (Z) of three different subtypes of TRLs, as previously described.[19,20] As well, following previously published protocols, plasma glycoprotein (Glyc-A, Glyc-B and Glyc-F) analysis was subjected to the same processing prior to NMR analysis.[15]

After isolation by ultracentrifugation of the TRL fraction from the plasma of the patients, samples were processed for the lipidomic study using NMR. With this technique, after extraction of the lipidic phase of the samples, up to 20 lipidic classes could be identified. Briefly, lipid extraction was performed using the BUME method.[21] This technique begins with a one-phase extraction of the samples in a butanol:methanol (BUME) mixture (3:1 v/v), followed by a two-phase extraction into heptane:ethyl acetate (3:1 v/v) using deionized water as a buffer. Because the approach is based on organic solvents with low density, the lipids are located in the upper phase, enabling their recovery and reducing the risk of contamination prior to NMR analysis. The NMR spectra were obtained in a Bruker Avance III 600 operating at 600.2 MHz frequency. The spectra processing was performed with the LipSpin software, a tool that can also deconvolute the lipid signals, obtaining the corresponding area (concentration) of each lipid class. (Figure S1).

2.5 | Culture of THP-1 monocytes and TRL stimulation conditions

Human THP-1 monocytes were obtained from ATCC and maintained in RPMI 1640 (Biowest Laboratories) supplemented with 10% (v/v) foetal bovine serum (FBS, Biowest Laboratories) and 1 mM penicillin–streptomycin. Cells were seeded at a cell density of 6×10^5 cells/well and differentiated into macrophages by incubation with 200 nM phorbol 12-mystrate 13-acetate (PMA, Sigma) for 72 h at 37°C with 5% CO_2. Before initiation of the experiments, cells were washed with PBS, followed by a 24-h incubation in RPMI 1640 10% FBS-supplemented medium.

Differentiated macrophages were then incubated in the presence of the isolated TRL-TG pools in serum-free medium: 10% v/v (increasing particle concentration) or the same particle concentration (40 nmol/L for per-particle cytokine secretion testing and 149.8 nmol/L for western blot experiments) at 4 and 24 h. TRL-induced cytotoxicity was tested with LDH assays (Roche) and was unaffected by TRL incubation. Lipopolysaccharide (LPS) at 10 ng/mL

in serum-free medium was used as a positive control as an inflammatory stimulus in the indicated experiments.

2.6 | Nile red staining

Cells were exposed to 100 ng/mL of the lipophilic fluorescent dye Nile Red (9-diethylamino-5H-benzo[α]phenoxazine-5-one, Sigma–Aldrich) diluted in PBS for 5 min at room temperature without prior fixation to visualise intracellular lipid droplets. Cell images were captured using an inverted microscope (Olympus IX71). To detect differences in lipid droplet accumulation after incubation with increasing quartiles of TRL-TG, fluorescence intensity was measured and quantified after adding 1% cholic acid (Sigma) in methanol for 1 h. Supernatants containing the solubilized fluorescence staining were placed in a fluorescence reader (Sinergy HT reader, Biotek), and intensity was detected at λ_{ex} 485/20 and λ_{em} 590/35.

2.7 | Cytokine quantification

The cell culture supernatant was stored at −80°C for later enzyme-linked immunosorbent assays (ELISAs). Following the corresponding manufacturer's instructions, ELISA kits for human IL-1β and TNF-α (R&D Systems) were used to measure the levels of these cytokines in the cell culture medium. A Sinergy HT reader (Biotek) was used to measure the absorbance at 450 nm.

2.8 | Quantitative real-time PCR

Total RNA was extracted from the differentiated macrophages using a PureLink RNA Mini Kit (Invitrogen). Following the manufacturer's instructions, the extracted RNA was reverse-transcribed to cDNA using random hexamers and the PrimeScript RT Reagent Kit (Takara Bio). Real-time PCR amplifications in a LightCycler 96 (Roche) for human IL-1β, TNF-α, IL-6 and CD206 were performed using TaqMan (Life Technologies) primers that were acquired from validated and predesigned Assays-on-Demand kits (Applied Biosystems). The $2^{\Delta\Delta C_t}$ was calculated to estimate the mRNA expression for each gene and sample, and GAPDH was used as a housekeeping gene to normalise the results of the genes of interest.

2.9 | Western blot analysis

Cells were lysed in RIPA buffer (0.1% SDS, 150 mM NaCl, 1% Nonidet P40, 50 mM Tris–HCl, 0.5% deoxycholate) containing phosphatase and protease inhibitors (Roche Diagnostics). Protein concentrations were measured using a Bradford Assay Kit (Bio-Rad). The iBlot® Dry Blotting System (Life Technologies) was used to transfer 20 μg of total protein to nitrocellulose membranes after separation on 10% SDS–PAGE gels (Cell Signaling Technology, Inc.). Antibodies against phospho P38 MAPK (Thr180/Tyr182), total P38 MAPK, phospho 44/42 MAPK (Thr202/Tyr204 and Thr185/Tyr187), total MAPK (Erk1/2), phospho NFκB P65, total NFκB P65, phospho-AKT (Ser473), total AKT, caspase-1 and GAPDH (Cell Signaling Technology, Inc.) were used. Membranes were incubated with the corresponding HRP-conjugated secondary antibodies (Dake), and bands were visualised using ECL detection reagents (Amersham™). Utilising ImageJ software, band intensities were measured, and densities were normalised to the total nonphosphorylated protein or GAPDH when corresponding.

2.10 | Statistical analysis

The Kolmogorov–Smirnov test was used to assess normality. For the clinical data presented, categorical variables are given as percentages, and nonnormally distributed continuous variables are shown as medians, 25th and 75th percentiles (IQR), or means and standard deviations (SD) when normally distributed. Differences between groups were analysed using the χ^2 test for categorical variables and the *t*-test and Kruskal–Wallis test for continuous variables. Additionally, Bonferroni correction for multiple comparisons was used when indicated. For the in vitro experimental analysis, the results are shown as the mean and SEM of at least three separate experiments. Bonferroni or Dunn's multiple comparisons tests were used to compare quartile differences (the corresponding analyses are shown in each figure legend). IBM SPSS Statistics (version 28.0.0.0) and GraphPad Prism 6.01 software (GraphPad Software Inc.) were used to conduct all statistical analyses. Statistically significant differences were indicated by $p < .05$.

3 | RESULTS

3.1 | Participant characteristics

The clinical, anthropometric and biochemical characteristics of the individuals included in the study, which were divided into quartiles of increasing TRL-TG concentrations, are summarised in Table 1. The group of patients with high concentrations of TRL-TG included younger participants, fewer women and more patients with obesity, T2DM and hypertension. The slight

TABLE 1 Clinical, anthropometric and biochemical characteristics of the 307 individuals of the study grouped by quartiles of TRL-TG.

	Quartiles of TRL-TG					
	Q1	**Q2**	**Q3**	**Q4**		
Number of participants	**78**	**76**	**77**	**76**		
TRL-TG concentration range, mmol/L	**.08–0.61**	**.62–0.97**	**.98–1.65**	**1.66–14.85**		
TRL-TG concentration range, mg/dL	**7.09–54.03**	**54.91–85.91**	**86.8–146.14**	**147.03–1315.37**		
Clinical, anthropometrical and imaging data					*p* Values	Adjusted *p* values
Age, years	61 (52–66)	63 (56–68)	60 (50–65)	55 (49–62)	<.001	–
Women, %	53.8	68.4	42.9	32.9	<.001	–
Obesity, %	42.9	56.6	69.7	65.8	.004	–
Type 2 diabetes, %	64.1	75	72.7	84.2	.042	–
Hypertension, %	42.3	60	64.5	54.1	.035	–
Cardiovascular disease, %	9	17.1	13	14.5	.511	.677
Plaque, %	31.1	34.2	44.6	39.7	.337	.936
IMT, mm	.72 (.64–0.78)	.69 (.64–.8)	.69 (.64–.76)	.68 (.61–.79)	.806	.352
Physical measurements						
BMI, kg/m^2	28.91 (26.36–33.73)	30.67 (28.2–36.5)	31.59 (29.47–36.94)	32.68 (29.16–35.8)	<.001	.288
Waist circumference (cm)	98 (90.5–108)	105 (95–116)	104 (101–113)	109 (100–114)	<.001	.054
Systolic BP, mmHg	132 (125–147)	135 (125–149)	139 (130–150)	141 (131–153)	.014	.115
Diastolic BP, mmHg	79 (71–83)	79 (70–83)	82 (77–90)	84 (78–90)	<.001	.074
Biochemical data						
Total cholesterol, mmol/L	5.01 (4.42–5.64)	5.57 (4.89–6.35)	5.8 (5.15–7)	6.56 (5.52–7.55)	<.001	<.001
Triglycerides, mmol/L	.92 (.76–1.07)	1.5 (1.36–1.71)	2.18 (2.02–2.65)	4.33 (3.47–5.48)	<.001	<.001
VLDL-C, mmol/L	.4 (.29–.5)	.74 (.6–.88)	1.11 (.93–1.25)	1.74 (1.34–2.44)	<.001	<.001
LDL-C, mmol/L	3.35 ± .89	3.8 ± 1	3.84 ± 1.15	3.15 ± 1.23	<.001	.001
HDL-C, mmol/L	1.29 (1.06–1.55)	1.18 (.95–1.34)	1.06 (.91–1.21)	1.01 (0.86–1.18)	<.001	<.001
Apo B-100, mg/dL	100 (84–117)	118 (101.5–138)	127 (108–149)	126.5 (101.5–156)	<.001	<.001
Apo A-I, mg/dL	131 (106–144)	121.5 (104–140.5)	120 (106–131)	116 (106.5–129.5)	.060	.239
Apo C-III, mg/dL	7.8 (5.2–10)	10.8 (8.3–13.4)	14.74 (11.9–17.8)	22.15 (18–25.7)	<.001	<.001
Glucose, mg/dL	119.5 (95–158)	123.6 (106–148.5)	132 (111–165)	152.1 (125.5–188.6)	<.001	.026
HbA1c, %	6.95 (5.6–7.7)	6.3 (5.5–7)	6.3 (5.6–7.3)	6.3 (5.7–7.4)	.152	.153
hsCRP, mg/L	1.65 (1.06–3.76)	2.24 (1.4–3.64)	2.34 (1.42–3.46)	2.44 (1.28–3.75)	.321	.942

Note: Data are presented as percentages (%) for categorical variables, means ± SDs for normally distributed continuous variables or medians (interquartile range) for nonparametric continuous variables. Statistical analysis: *p* values from the χ^2 test for categorical variables and the *t* test or Kruskal–Wallis test for continuous variables. Adjusted *p* values were controlled by age, sex, obesity, diabetes and hypertension.

Abbreviations: Apo A-I, apolipoprotein AI; Apo B-100, apolipoprotein B100; Apo C-III, apolipoprotein CIII; BMI, body mass index; diastolic BP, diastolic blood pressure; HbA1c, glycated haemoglobin; HDL-C, HDL cholesterol; hsCRP: high-sensitivity C-reactive protein; IMT, intima-media thickness; LDL-C, LDL cholesterol; systolic BP, systolic blood pressure; VLDL-C: VLDL cholesterol.

increase in the number of patients with T2DM was accompanied with similar HbA1c levels. In addition, patients with T2DM using hypoglycaemic drugs were 84%, 83%, 79% and 70% according to quartiles of increasing TRL-TG ($p = .266$). In addition, patients in the highest quartile of TRL-TG exhibited greater BMI, waist circumference, systolic blood pressure (SBP) and diastolic blood pressure (DBP); these associations were lost when adjusting the *p* values by age, sex, obesity, T2DM and hypertension. There were no statistical differences in the prevalence of cardiovascular disease, carotid atherosclerotic plaque and IMT. Plasma biochemical

examination revealed an increase in total cholesterol, TGs, VLDL-C, Apo B-100, Apo C-III and glucose in the highest TRL-TG groups. In these groups, patients had lower LDL-C and HDL-C levels. These biochemical associations remained robust after adjusting for the mentioned covariates. A trend towards higher hsCRP levels was observed, but this association was not significantly different between groups.

3.2 | Plasma and TRL characterization by NMR

The NMR-determined metabolomic profile of the individuals grouped by quartiles of TRL-TG is shown in Figure 1. Growing quartiles of TRL-TG showed an increase in the plasma concentrations of all the different NMR-measured TRL particles (large, medium, small and total TRL particles) with respect to each quartile after Bonferroni-adjusted multiple comparisons ($p < .001$, Figure 1A), with statistically positive Spearman correlations ($p = .848$ for large TRL-P, $p = .858$ for medium TRL-P, $p = .862$ for small TRL-P and $p = .865$ for total TRL-P; $p < .001$). Regarding NMR-measured TRL particle diameter, larger diameters were observed in Q1 and Q4, and Q4 had the largest diameter values ($p < .001$, Figure 1A). However, these correlations were not statistically significant ($p = .105$, $p = .067$). Comparable to TRL particles, a higher content of TG on TRL was associated with increasing plasma levels of NMR-measured glycoprotein acetyls (Glyc-A, Glyc-B and Glyc-F, $p < .05$, Figure 1B), which are markers of chronic inflammation, and all of these associations had a positive Spearman correlation ($p = .785$ for Glyc-A, $p = .530$ for Glyc-B and $p = .795$ for Glyc-F; $p < .001$). Only a slight, significant correlation was found between TRL particle diameter and Glyc-F ($p = .159$; $p = .005$). Additionally, we analysed the association between TRL-TG and glycoproteins according to presence or absence of atherosclerotic plaque. The results did not reveal significant differences between those with atherosclerotic plaque than those without. This might be due to the relatively small sample size within each group and the low prevalence of outcomes.

The NMR-determined lipidomic analysis of the isolated TRL-containing fraction of the participants grouped in TRL-TG quartiles is shown in Figure 2. The per-particle relative composition of each quartile of patients showed changes in their lipid distribution. TRL-TG enrichment was accompanied by a significantly reduced relative content of cholesterol (both free and esterified; $p < .001$) and phospholipids (including sphingomyelin, phosphatidylcholine, lysophosphatidylcholine and glycerophospholipids; $p < .01$) present in TRLs (Figure 2A). The NMR lipidomic analysis of the fatty acid families present in this fraction showed that particles become significantly enriched in omega-9 fatty acids ($p < .001$) and depleted in SFAs ($p < .001$) as the TRL-TG content increases (Figure 2B). Additionally, the relative particle content in oleic acid increased ($p < .001$) as the linoleic acid and ARA + EPA content in particles decreased ($p < .001$, Figure 3C).

3.3 | TRL uptake by differentiated macrophages and cytokine secretion

TRLs isolated from 144 representative individuals in the Q1, Q2, Q3 and Q4 groups were pooled for incubation with THP-1-derived macrophages. In vitro, macrophages were treated with 10% v/v TRL-TG pools, and Nile red staining was performed. Accumulation of lipid droplets after 24 h of incubation was imaged by phase contrast and fluorescence microscopy (Figure 3A). There was an increase in the number of cytoplasmic lipid droplets in the cells treated with the TRL-TG pools (black arrows and orange–yellow fluorescent droplets in Figure 3A). Cytoplasmic lipid content quantification after dye extraction with cholic acid (graph in Figure 3A) showed an increase in the accumulation of lipids within the cells incubated with the TRL-TG pools (TRL pools RFU versus untreated control cells, $p < .05$), and there were no differences between each group after multiple comparisons analysis.

After TRL internalisation, THP-1-derived macrophages exposed to growing TRL-TG pools demonstrated an increase in the secretion of cytokines into the extracellular media (Figure 3B). At the time points tested, the 4-h incubation with TRL pools did not result in a significant increase in the release of the pro-inflammatory cytokines IL-1β and TNF-α compared to that in untreated control cells, but their secretion was induced by LPS. After 24 h of treatment, there was a time-dependent response of IL-1β and TNF-α secretion compared to 4 h (#$p < .05$) when stimulated by LPS and three of the TRL pools. At this 24-h time point, increased secretion was also observed in LPS- and TRL-treated cells compared to control cells (*$p < .05$). Multiple comparison tests showed that there were differences between pools in the release of both cytokines after 24 h of incubation (*$p < .05$ indicated by boxes in Figure 3B). The mean particle concentration (TRL-P) in each pool is indicated in the table of Figure 3B. Next, the expected per-particle secretion of cytokines in the TRL-treated cells was calculated by correcting for total TRL particles measured with NMR (that is, picograms of each secreted cytokine divided by nmol of TRL particles on each pool). On this basis, both IL-1β and TNF-α secreted levels were higher in the pools containing a lower

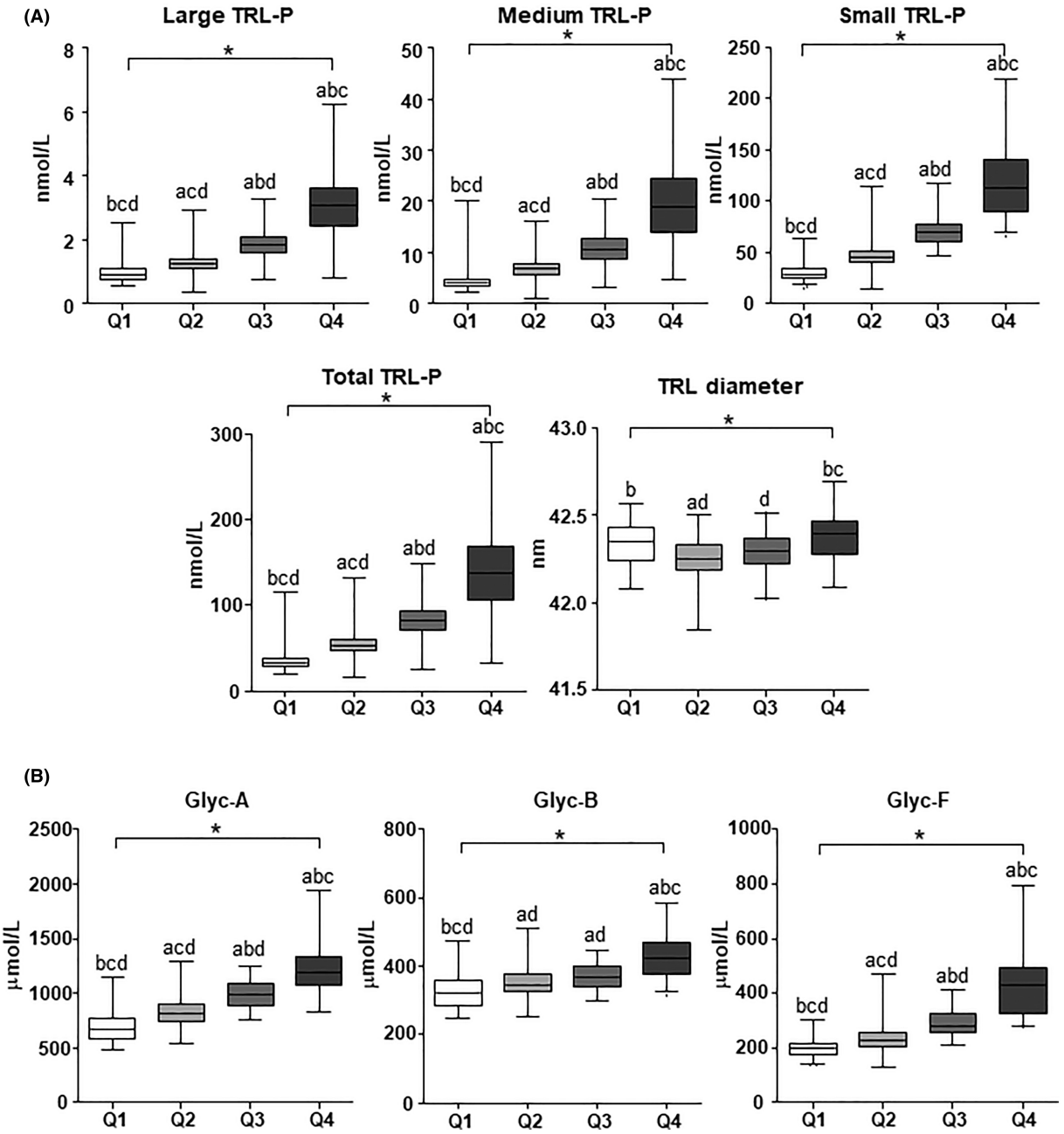

FIGURE 1 NMR-measured plasma TRL and glycoprotein concentrations of the study participants grouped into quartiles of TRL-TG. The plasma concentrations of all-sized and total TRL and TRL diameter (A) and different glycoproteins (B) in the study participants grouped by TRL-TG quartiles are shown in the boxplots. All parameters shown were measured by NMR. Statistical differences between quartiles are indicated by different letters (a, b, c and d) above the boxplots from Bonferroni adjustment for multiple comparisons of the Kruskal–Wallis test: a, $p < .05$ vs. Q1; b, $p < .05$ vs. Q2; c, $p < .05$ vs. Q3; d, $p < .05$ vs. Q4. *$p < .001$ indicates the adjusted total differences between quartiles controlled by age, sex, obesity, type 2 diabetes and hypertension. Glyc-A: glycoprotein A; Glyc-B: glycoprotein B; Glyc-F: glycoprotein F. Quartiles of TRL-TG in mmol/L: Q1, .08–.61; Q2, .62–.97; Q3, .98–1.65; Q4, 1.66–14.85.

percentage of TG and a higher percentage of cholesterol and phospholipids (Figure 3C).

To confirm the per-particle cytokine secretion, THP-1-derived macrophages were incubated for 24 h with pools containing the same TRL particle concentrations (40 nmol/L) but different TG, cholesterol and phospholipid contents (percentage). The cytokine release of both IL-1β and TNF-α was increased in the pools with a lower TG percentage and higher cholesterol and phospholipid percentages (Figure S2).

To confirm that these cytokine release effects were not due to cell death upon TRL incubation, cytotoxicity was tested by LDH release into the medium, which was unaltered by the TRL pools (data not shown).

(A)

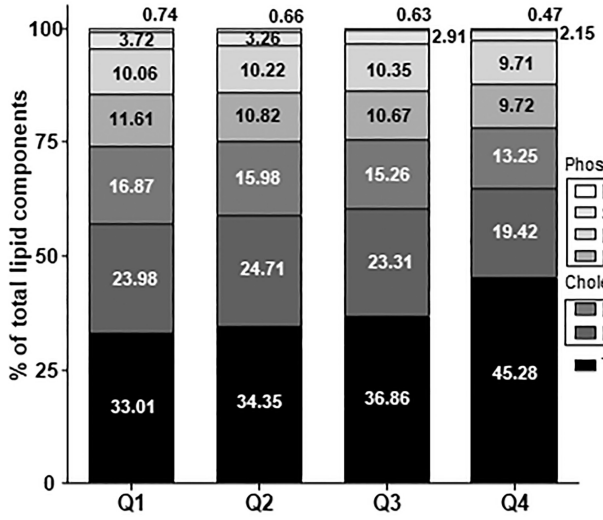

Bonferroni adjusted p-values

Main lipid components

	Q1 vs Q2	Q1 vs Q3	Q1 vs Q4	Q2 vs Q3	Q2 vs Q4	Q3 vs Q4
LPC	0.98	0.349	<0.001	1	0.007	0.035
SM	<0.001	<0.001	<0.001	<0.001	<0.001	<0.001
PL	0.827	0.334	0.772	1	0.017	0.004
PC	0.002	<0.001	<0.001	1	<0.001	<0.001
FC	0.037	<0.001	<0.001	0.026	<0.001	<0.001
EC	1	1	<0.001	0.134	<0.001	<0.001
TG	0.647	<0.001	<0.001	0.017	<0.001	<0.001

(B)

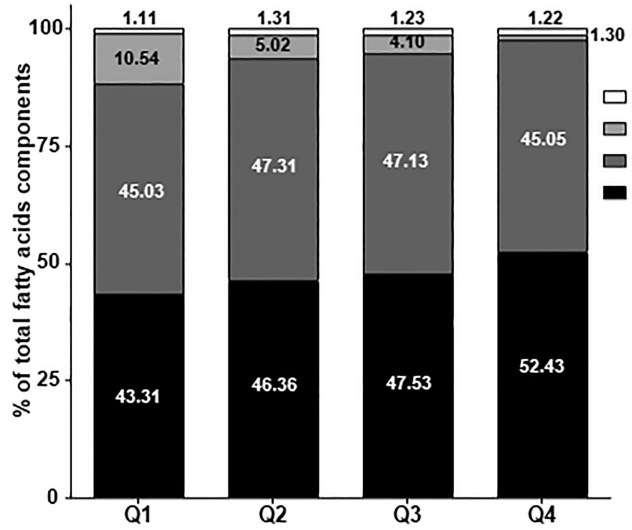

Fatty acid families

	Q1 vs Q2	Q1 vs Q3	Q1 vs Q4	Q2 vs Q3	Q2 vs Q4	Q3 vs Q4
Ω-3	0.055	0.206	1	1	0.097	0.33
SFA	<0.001	<0.001	<0.001	0.366	<0.001	<0.001
Ω6+7	0.25	0.36	1	1	0.265	0.38
Ω9	0.004	<0.001	<0.001	1	<0.001	<0.001

(C)

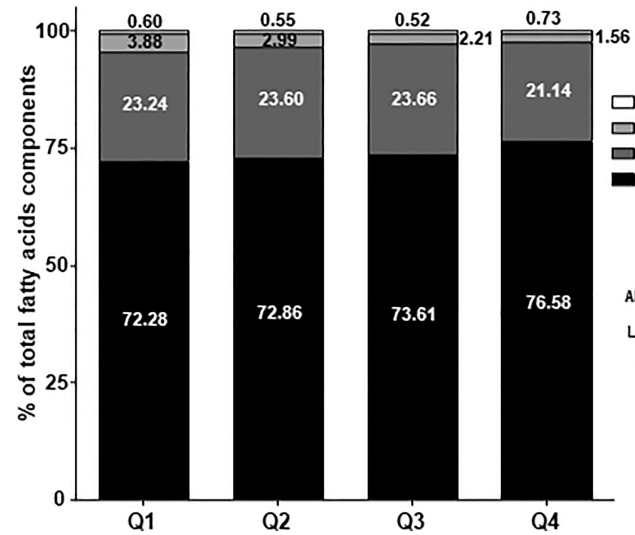

Fatty acid species

	Q1 vs Q2	Q1 vs Q3	Q1 vs Q4	Q2 vs Q3	Q2 vs Q4	Q3 vs Q4
DHA	1	1	1	1	0.892	1
ARA+EPA	0.082	<0.001	<0.001	0.008	<0.001	0.001
Linoleic	1	1	0.012	1	0.002	0.001
Oleic	1	0.616	<0.001	1	<0.001	0.002

FIGURE 2 NMR lipidomic characterization of the TRL-containing fraction isolated from the grouped study participants. The mean per-particle TRL relative lipidomic composition is shown. Bars on the left panels represent the mean percentage of the indicated lipid of the total lipid content within the fraction (A), the mean percentage of the indicated fatty acid families (B), and the indicated fatty acids species (C). Tables on the right show the Bonferroni-corrected p values for multiple comparisons of the Kruskal–Wallis test between quartiles (Q1–Q4). $p < .05$ was considered statistically significant, and those variables with significant changes are written in bold. ARA + EPA, arachidonic acid and eicosatetraenoic acid; DHA, docosahexaenoic acid; EC, esterified cholesterol; FC, free cholesterol; Linoleic, linoleic acid; LPC, lysophosphatidylcholine; Oleic, oleic acid; PC, glycerophospholipids; PL, phosphatidylcholine; SFA, saturated fatty acids; SM, sphingomyelin; TGs, triglycerides; Ω-3, omega-3 fatty acids; Ω6 + 7, omega-6 + 7 fatty acids; Ω-9, omega-9 fatty acids. Quartiles of TRL-TG in mmol/L: Q1, .08–.61; Q2, .62–.97; Q3, .98–1.65; Q4, 1.66–14.85.

3.4 | mRNA expression of inflammatory genes and pathways implicated

Incubation of THP-1-derived macrophages with TRL pools modified the expression of different proinflammatory. A 4-h incubation with TRL pools increased the expression of the proinflammatory genes *IL1B* and *TNFA*, (*$p < .05$ compared to untreated control cells). *TNFA* was also significantly upregulated by LPS stimulation, (Figures 4A,B). For the two pro-inflammatory genes (Figure 3A–C), time differences were observed after 24-h incubation. At this time point, gene expression was reduced compared to 4 h (#$p < .05$) and compared to its control (*$p < .05$). After multiple comparisons, no differences were observed between TRL-treated cells in the expression of any of the genes tested at any of the time points.

Next, we tested whether the TRL-induced inflammatory responses were partially mediated by TRL-4-related Akt/NF-κB and MAPK activation (Figure 4C). Four hours of treatment with LPS (10 ng/mL) induced the phosphorylation of Erk1/2 (*$p < .05$ compared to control), whereas incubation with TRL did not modify the intracellular phosphorylation of any of the proteins investigated. The 24-h incubation with LPS diminished Erk1/2 activation (#$p < .05$ compared to 4-h treatment) and induced the activation of p38, NF-κB-p65 and Akt (*$p < .05$ compared to untreated control cells). At this time point, incubation with TRL elicited the phosphorylation of p38, NF-κB-p65 and Akt ($p < .05$ compared to control cells), and the phosphorylation of Erk1/2 decreased over time (#$p < .05$ compared to 4-h treatment).

Inflammasome activation is the likely mechanism underlying IL-1β secretion; hence, the expression of caspase-1 was examined to test inflammasome stimulation (Figure 4D). A 4-h LPS treatment induced the expression of mature caspase-1 (p20), which was unaltered by TRL treatment. After 24 h, LPS induced the expression of both pro-caspase-1 (p45) and p20, whereas TRL treatment only induced the expression of p45 (*$p < .05$ compared to control cells).

4 | DISCUSSION

In the present study, we explored the associations between TRL, systemic inflammation and TRL-mediated inflammatory effects in macrophages according to the TRL-TG levels of 307 individuals with hyperlipidemia at metabolic risk. The burden of atherosclerotic disease (cardiovascular disease, carotid atherosclerotic plaque and IMT) showed no differences across TRL-TG quartiles, probably because of the small sample size per group and low outcome prevalence. As expected, TG enrichment of TRL was associated with increased plasma concentrations of TRL particles. High TG concentrations were also associated with higher plasma levels of glycoproteins, which are markers of chronic inflammation, as assessed by ^{1}H-NMR. Moreover, TRLs isolated from patients revealed changes in the composition leading to different pro-inflammatory cytokine secretion patterns in vitro. Macrophages treated with TRLs that had a higher proportion of TG secreted less IL-1β and TNF-α, whereas those containing higher cholesterol and phospholipid levels demonstrated increased cytokine release.

The mechanisms linking TRL and inflammation have been studied recently.[10,22,23] In our study, patients in the highest quartile of TRL-TG showed higher levels of TRL particles as well as Glyc-A, B and F. Recently, we and others have provided evidence that these liver-derived glycoproteins are reliable biomarkers of low-grade systemic inflammation in different conditions, including infectious and autoimmune diseases, T2DM, hypertension and atherosclerotic cardiovascular disease.[15,16,24–27] The robustness of these NMR-measured glycoproteins improves the detection of systemic inflammation to a wider extent than single markers, such as high-sensitivity CRP.[19,28] In our study, we could not detect differences in this clinically established marker, whereas the concentrations of Glyc-A, B and F increased in parallel to TRL-TG levels. These results suggest that TRL concentrations and composition have a significant impact on the subclinical inflammatory status of patients with lipid metabolism derangements.

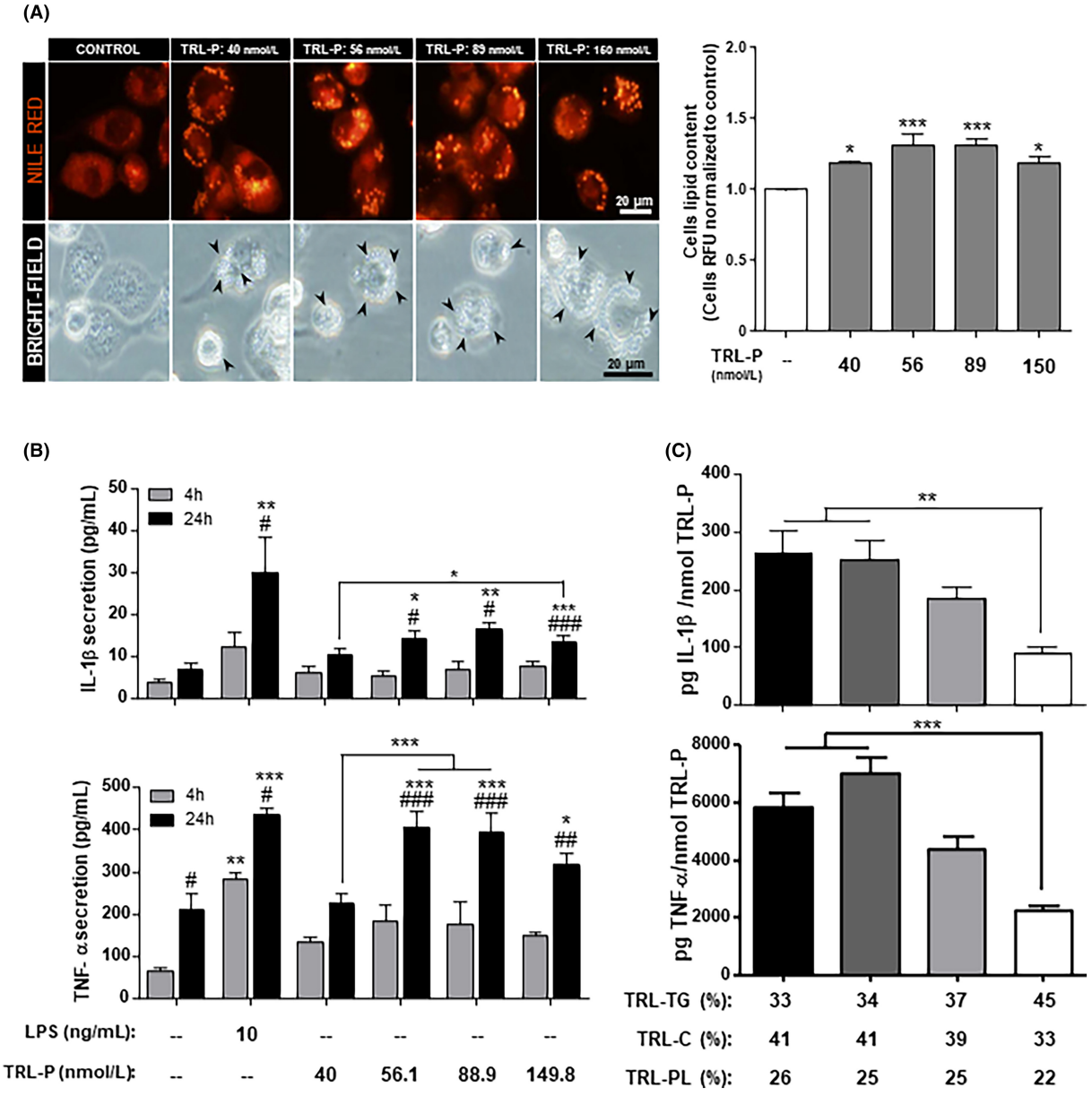

FIGURE 3 Incubation with isolated TRL induced lipid accumulation and cytokine secretion in THP-1-derived macrophages. (A, B) THP-1 macrophages were incubated with 10% v/v TRL-P (nmol/L) and 10 ng/mL LPS or untreated for lipid accumulation and cytokine secretion. (A) Representative images from three experiments are shown after 24 h of incubation and Nile red staining or in the bright field of an inverted microscope. Lipid droplets after TRL treatment with the particle concentration range indicated on top of the images were stained in yellow–orange for Nile Red images or indicated by black arrows in bright field images photographed at 400× magnification. Lipid accumulation after Nile red solubilization and quantification is shown on the graph. The bars represent the mean + SEM (error bars) of the indicated treatment's relative fluorescent units (RFU) normalised to untreated control cells. *$p < .05$, **$p < .001$ from Kruskal–Wallis Dunn's multiple comparison compared to control cells. (B) Cell culture media were analysed for IL-1β and TNF-α secretion by ELISA after 4 (grey bars) and 24 h (black bars) of incubation. Bars represent the mean + SEM (error bars) secretion after the treatment indicated below, and the *p* values from two-way ANOVA with Bonferroni multiple compassion tests are as follows: #$p < .05$, ##$p < .01$, ###$p < .001$ from incubation time differences (24 h vs. 4 h); *$p < .05$, **$p < .01$, ***$p < .001$ from treatment (LPS or TRL) compared to untreated control cells. (C) Expected IL-1β and TNF-α secretion into the cell media divided by the mean TRL particle concentration of each group is shown as the picograms of each cytokine per nmol of TRL (pg/nmol). Bars represent the mean + SEM (error bars). Cytokine secretion and triglyceride, cholesterol and phospholipid mean percentages contained in the particles are shown in the table below. *$p < .05$ from Kruskal–Wallis with Dunn's multiple comparison test. The results from three experiments run in duplicate are shown. LPS, lipopolysaccharide; TRL-C, TRL cholesterol; TRL-P, TRL particle concentration; TRL-PL, TRL phospholipids; TRL-TG, TRL triglycerides.

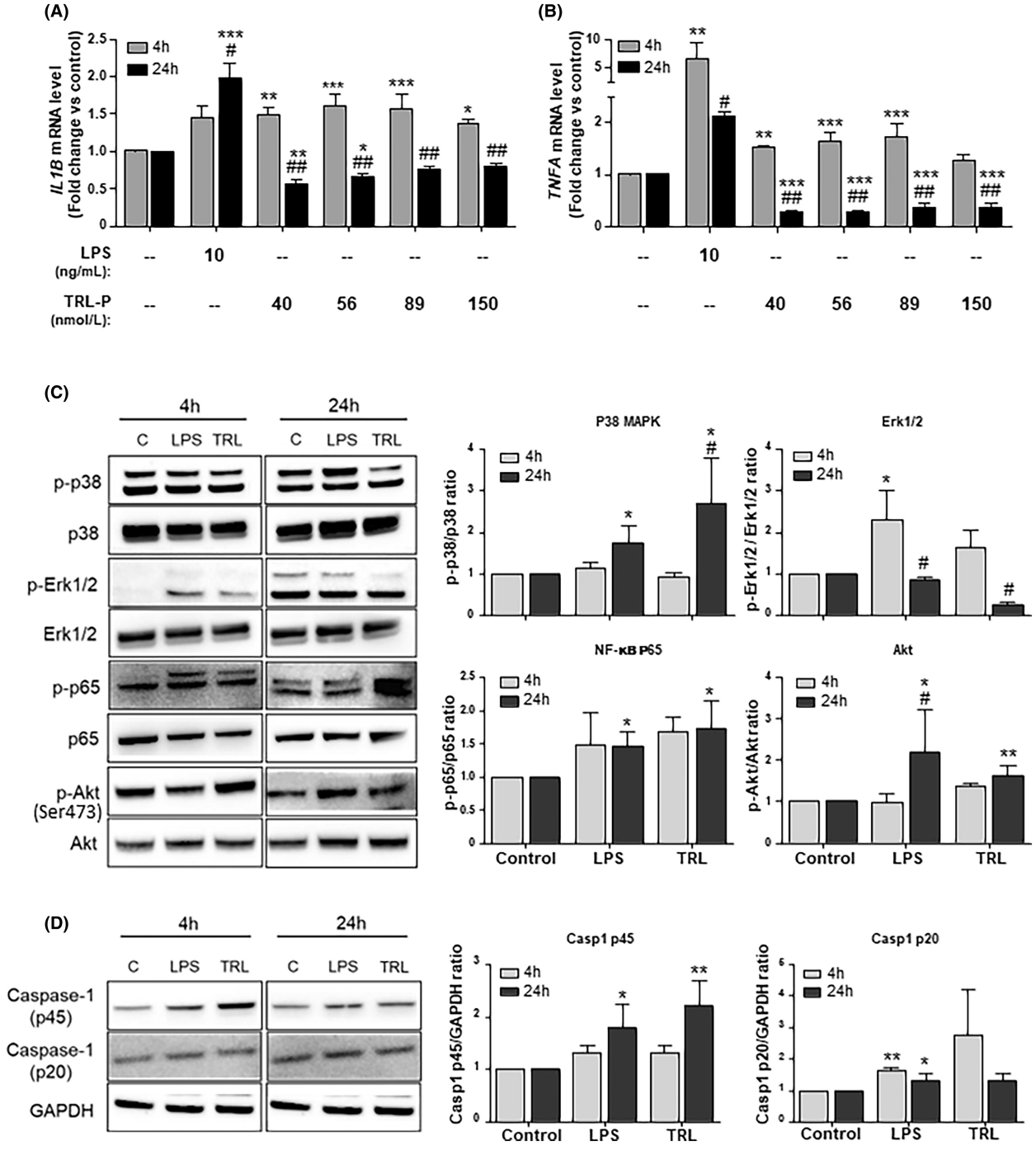

FIGURE 4 Effects of TRL incubation on cytokine mRNA expression, protein phosphorylation and caspase-1 expression. (A–D) Fold change in the mRNA expression of cytokines in THP-1-derived macrophages. Cells were cultured with LPS (10 ng/mL) as a positive control for the expression of proinflammatory cytokines or with pools of isolated TRL at 10% v/v (with the particle concentrations indicated) for 4 (grey bars) and 24 h (black bars). Gene expression levels of IL1B (A) and TNFA (B) were normalised to GAPDH and expressed as the mean (bars) + SEM (error bars) fold increase compared to untreated cells from four experiments run in duplicate. (C, D) THP-1-derived macrophages were treated with 10 ng/mL LPS or TRL (149.8 nmol/L) for 4 (light-grey bars) and 24 h (dark-grey bars). Representative Western blot images for p38, Erk1/2, NF-κB-p65 and Akt phosphorylation (C) and procaspase-1 p45 and mature p20 caspase-1 expression (D) are shown in the left panels. Data on the graphs are expressed as the fold increase compared to untreated control cells, and bars show the mean + SEM ratios of the phosphorylated form of each protein to its total protein levels for Akt/NF-κB and MAPK and the ratio to GAPDH for caspase-1 (p45 and p20). The results from three experiments run in duplicate are shown. *p* Values from two-way ANOVA with Bonferroni multiple comparison tests are as follows: #$p < .05$, ##$p < .001$ from incubation time differences (24 h vs. 4 h); *$p < .05$, **$p < .01$, ***$p < .001$ from treatment (LPS or TRL) compared to untreated control cells.

The biochemical composition of the TRL might be an important factor in the mediation of inflammation. For instance, the plasma levels of Apo C-III, an important apolipoprotein implicated in TRL arterial binding and retention that is associated with inflammation,[9,29] increased with increasing concentrations of TRL-TG in the study patients. We also detected specific modifications in the lipidome of the TRL, with the particles becoming depleted in cholesterol and phospholipids as their TG content increased, also modifying their fatty acid compositions of omega-9 and SFA. Whether these changes in the lipidome of the particles are responsible for the increased systemic inflammatory status remains unknown.

To evaluate the impact of TRL composition and particle number, we tested the responses mediated in THP-1-derived macrophages incubated with pools of isolated TRL in vitro. Lipid accumulation in macrophages was augmented after TRL incubation. Additionally, this lipid accumulation resulted in the secretion of the pro-inflammatory cytokines IL-1β and TNF-α. Our results indicate the importance of particle number when explaining inflammation, as higher particle concentrations increase cytokine secretion. However, the per-particle analysis revealed that particle composition is also important, since we detected differences in cytokine release depending on the percentages of TG, cholesterol and phospholipids, with higher cytokine secretion when cholesterol and phospholipid content were higher. Interestingly, Q1 TRL, which had the higher proinflammatory effect per particle, had a higher proportion of SFA and less W9. Moreover, apoCIII was increased across TRL-TG quartiles and could also have an impact on inflammation. These findings are in line with those reported in an observational large-cohort-based study published by Balling et al.,[30] where VLDL cholesterol but not VLDL triglycerides explained one-half of myocardial infarction risk. The complete lipidome analysis of our study showed that the fatty acid composition associated with the increased release of cytokines includes those particles with lower omega-9 and higher SFA percentages; reduced oleic acid content would also be associated with an increased release of cytokines. Thus, TRL particles with higher TG content (but less cholesterol) induce a lower inflammatory response in vitro (according to per-particle analysis of cytokine release in macrophages), while patients in the higher TRL-TG quartile had higher systemic inflammation (according to glycoprotein plasma levels). This paradox could be explained by the number of TRL and other atherogenic particles, which are higher in the TRL-TG Q4, as suggested by apoB concentrations and NMR data.

We observed increased gene expression of the proinflammatory genes *IL1B* and *TNFA* at an earlier time point, which was reduced after 24 h of incubation. However, this reduction in gene expression at 24 h was contrary to the increased phosphorylation of the Toll-like receptor (TLR)-related Akt/NF-kB and MAPK pathways, as well as procaspase-1 expression. These molecular factors modulate the nod-like receptor family pyrin domain-containing 3 (NLRP3) inflammasome, a complex that mediates IL-1β final maturation and secretion.[31] Our results suggest that TRLs train macrophages to secrete cytokines; however, as gene expression appears to be affected earlier than protein phosphorylation pathways, this activation might be cyclic or tightly regulated by the induction of anti-inflammatory genes, or that the phosphorylation of these proteins occurs concomitantly with the cytokine secretion. Further studies using specific inhibitors are required to confirm the implication of these pathways. Indeed, TRLs have already been shown to increase inflammatory genes, endothelial adhesion and ROS production and expression in vessel walls.[12,32] These effects vary depending on the fatty acid composition of the TRL, as those derived from olive oil-rich diets being less inflammatory than diets high in saturated fats.[33,34] Thus, in our study, particles triggered a molecular response that could be explained by different TRL components. The time-differential expression patterns we observed remain to be studied considering the physiological roles of the fatty acids, lipids and other components present in the TRL.

In line with our findings, association studies have shown that TG concentrations and remnant cholesterol are associated with the inflammatory status in patients to a better extent than LDL.[11,35] Therefore, published studies have provided evidence that TG and TRL are independent markers for an increased risk of cardiovascular disease.[5] Targeting TGs in patients at risk for heart disease has become a matter of current debate since the TG component of TRL does not seem to account for atherogenicity.[10] Research from the STRENGTH study (an omega-3-based treatment containing a high-dose (4 g/day) combination of eicosapentaenoic acid [EPA] and docosahexaenoic acid [DHA]) indicated a 20% decrease in TGs without any positive effects on clinical events.[36] In the randomised trial known as PROMINENT, the novel drug pemafibrate (0,4 mg/day) (a fibrate that acts as a PPAR-α agonist to reduce plasma TG levels) caused a 26% decrease in TG levels, but no reduction in rates of heart attack, stroke, or cardiovascular death over the follow-up period was reported.[37] In contrast, the REDUCE-IT trial (4 g/day) (icosapent ethyl (EPA)-based treatment) demonstrated a significant reduction in clinical events that accompanied TG reduction.[38] In these three high-quality clinical trials, with apparent opposite conclusions, a reduction in the inflammatory status followed TG reduction. On the other hand, the beneficial effects observed in the REDUCE-IT trial were independent of TG lowering and have been

attributed to direct effects of EPA on inflammation mediators, platelet aggregation or antioxidant effects that were not induced by the combination of EPA and DHA used in the STRENGHT study. However, pemafibrate, while reducing parameters associated with TRL, increases the LDL-C concentrations and atherogenic particles as assessed by apoB values, which is in accordance with our observations.

We reported, following both in vivo and in vitro approaches, the relevance of TRLs to the inflammatory status in patients at cardiovascular risk and to the inflammatory response mediated by macrophages, a key process in the development of atherosclerosis. A limitation of our study is that we could not go in depth into the molecular mechanisms that regulate this response, since our findings are observational when addressing the expression and modulation of the pro-inflammatory pathways. However, we have provided a detailed metabolomic and lipidomic profile of patients using ^{1}H-NMR technology, a reliable and modern method for assessing inflammatory diseases. We have provided a wide view that reflects a molecular signature of the patients, and we have used these patient-derived samples to study their effects in vitro. However, we used pools of patient-derived samples that could limit the individual effect of each patient. Finally, these results must be interpreted with caution when generalising the macrophage response to the systemic inflammatory status of patients.

In conclusion, we have characterised a cohort of patients at cardiovascular risk using ^{1}H-NMR, and we reported an association among their TRL-TG levels, their plasma TRL particles and a systemic inflammatory status. Here, we show how TG enrichment of their TRL modifies their lipidome, which exerts different cytokine secretion patterns. With higher particle concentrations causing higher cytokine secretion, our per-particle results suggest that the cholesterol and/or phospholipid components of the TRL are more proinflammatory than the TG component. Therefore, TRL particles, which can contain up to four times higher cholesterol content per particle than LDL particles, reflect a greater inflammatory status in those patients with increased particle numbers. This study supports the notion that evaluating TRL particle concentrations should be of clinical relevance in patients at cardiovascular risk and that the cholesterol and phospholipid contents carried by these lipoproteins play an important role in the inflammatory events that occur during atherosclerosis development.

ACKNOWLEDGEMENTS

We acknowledge all authors for their participation. JM-V: study design, data analysis and interpretation, article preparation, examination of the results and manuscript review. DL, RR-C, NP, NA: data analysis and results review. RR, YE: technical support and review. LM, DI, JG: research design, data analysis and interpretation, article preparation, review of the findings, manuscript review, overall study supervision and manuscript guarantors. We acknowledge the IISPV-BIOBANC for their assistance with sample processing, storage and custody. The authors thank the participants of the study for their contributions.

FUNDING INFORMATION

Grants from the Instituto de Salud Carlos III (ISCIII, Madrid, Spain) were used to support this work (PI18/00515). The Spanish Biomedical Research Centre in Diabetes and Associated Metabolic Disorders (CIBERDEM) jointly provided national funding. The European Regional Development Fund (ERDF) co-funded this project.

NA is CEO and co-founder of Biosfer Teslab SL.

CONFLICT OF INTEREST STATEMENT

The rest of the authors declare that there were no financial or commercial relations that may be viewed as potential conflicts of interest.

ORCID

Juan Moreno-Vedia https://orcid.org/0000-0002-2673-3822
Ricardo Rodríguez-Calvo https://orcid.org/0000-0001-7513-0983
Lluís Masana https://orcid.org/0000-0002-0789-4954
Daiana Ibarretxe https://orcid.org/0000-0002-5442-1930
Josefa Girona https://orcid.org/0000-0002-6267-8779

REFERENCES

1. Ference BA, Ginsberg HN, Graham I, et al. Low-density lipoproteins cause atherosclerotic cardiovascular disease. 1. Evidence from genetic, epidemiologic, and clinical studies. A consensus statement from the European atherosclerosis society consensus panel. *Eur Heart J*. 2017;38:2459-2472. doi:10.1093/eurheartj/ehx144
2. Borén J, John Chapman M, Krauss RM, et al. Low-density lipoproteins cause atherosclerotic cardiovascular disease: pathophysiological, genetic, and therapeutic insights: a consensus statement from the European atherosclerosis society consensus panel. *Eur Heart J*. 2020;41:2313-2330. doi:10.1093/EURHEARTJ/EHZ962
3. Sampson UK, Fazio S, Linton MF. Residual cardiovascular risk despite optimal LDL-cholesterol reduction with statins: the evidence, etiology, and therapeutic challenges. *Curr Atheroscler Rep*. 2012;14:1-10. doi:10.1007/S11883-011-0219-7
4. Ginsberg HN, Packard CJ, Chapman MJ, et al. Triglyceride-rich lipoproteins and their remnants: metabolic insights, role in atherosclerotic cardiovascular disease, and emerging therapeutic strategies-a consensus statement from the European

atherosclerosis society. *Eur Heart J*. 2021;42:4791-4806. doi:10.1093/EURHEARTJ/EHAB551
5. Nordestgaard BG, Varbo A. Triglycerides and cardiovascular disease. *The Lancet*. 2014;384:626-635. doi:10.1016/S0140-6736(14)61177-6
6. Padro T, Muñoz-Garcia N, Badimon L. The role of triglycerides in the origin and progression of atherosclerosis. *Clinica e Investigacion En Arteriosclerosis*. 2021;33:20-28. doi:10.1016/J.ARTERI.2021.02.007
7. Johansen MØ, Vedel-Krogh S, Nielsen SF, Afzal S, Davey Smith G, Nordestgaard BG. Per-particle triglyceride-rich lipoproteins imply higher myocardial infarction risk than low-density lipoproteins: Copenhagen general population study. *Arterioscler Thromb Vasc Biol*. 2021;41:2063-2075. doi:10.1161/ATVBAHA.120.315639
8. Mahley RW, Huang Y. Atherogenic remnant lipoproteins: role for proteoglycans in trapping, transferring, and internalizing. *J Clin Invest*. 2007;117:94-98. doi:10.1172/JCI30889
9. Olin-Lewis K, Krauss RM, La Belle M, et al. ApoC-III content of apoB-containing lipoproteins is associated with binding to the vascular proteoglycan biglycan. *J Lipid Res*. 2002;43:1969-1977. doi:10.1194/JLR.M200322-JLR200
10. Nordestgaard BG. Triglyceride-rich lipoproteins and atherosclerotic cardiovascular disease: new insights from epidemiology, genetics, and biology. *Circ Res*. 2016;118:547-563. doi:10.1161/CIRCRESAHA.115.306249
11. Hansen SEJ, Madsen CM, Varbo A, Nordestgaard BG. Low-grade inflammation in the association between mild-to-moderate hypertriglyceridemia and risk of acute pancreatitis: a study of more than 115,000 individuals from the general population. *Clin Chem*. 2019;65:321-332. doi:10.1373/CLINCHEM.2018.294926
12. Wu HM, Ni XX, Xu QY, Wang Q, Li XY, Hua J. Regulation of lipid-induced macrophage polarization through modulating peroxisome proliferator-activated receptor-gamma activity affects hepatic lipid metabolism via a toll-like receptor 4/NF-κB signaling pathway. *J Gastroenterol Hepatol*. 2020;35(11):1998-2008. doi:10.1111/jgh.15025
13. Schwartz EA, Reaven PD. Lipolysis of triglyceride-rich lipoproteins, vascular inflammation, and atherosclerosis. *Biochim Biophys Acta*. 2012;1821:858-866. doi:10.1016/J.BBALIP.2011.09.021
14. Otvos JD, Shalaurova I, Wolak-Dinsmore J, et al. GlycA: a composite nuclear magnetic resonance biomarker of systemic inflammation. *Clin Chem*. 2015;61:714-723. doi:10.1373/clinchem.2014.232918
15. Amigó N, Fuertes-Martín R, Malo AI, et al. Glycoprotein profile measured by a 1H-nuclear magnetic resonance based on approach in patients with diabetes: a new robust method to assess inflammation. *Life (Basel)*. 2021;11:1407. doi:10.3390/LIFE11121407
16. Andreychuk N, Llop D, Moreno-Vedia J, et al. Glycoprotein serum concentrations assessed by ^{1}H-NMR are increased in patients with high blood pressure. *Hypertension*. 2022;80:460-469. doi:10.1161/HYPERTENSIONAHA.122.20137
17. Havel RJ, Eder HA, Bragdon JH. The distribution and chemical composition of ultracentrifugally separated lipoproteins in human serum. *J Clin Invest*. 1955;34:1345-1353. doi:10.1172/JCI103182
18. Mallol R, Amigó N, Rodríguez MA, et al. Liposcale: a novel advanced lipoprotein test based on 2D diffusion-ordered 1H NMR spectroscopy. *J Lipid Res*. 2015;56:737-746. doi:10.1194/jlr.D050120
19. Moreno-Vedia J, Rosales R, Ozcariz E, et al. Triglyceride-rich lipoproteins and glycoprotein a and B assessed by ^{1}H-NMR in metabolic-associated fatty liver disease. *Front Endocrinol (Lausanne)*. 2022;12:775677. doi:10.3389/FENDO.2021.775677
20. Rodríguez-Borjabad C, Ibarretxe D, Girona J, et al. Lipoprotein profile assessed by 2D-^{1}H-NMR and subclinical atherosclerosis in children with familial hypercholesterolaemia. *Atherosclerosis*. 2018;270:117-122. doi:10.1016/J.ATHEROSCLEROSIS.2018.01.040
21. Löfgren L, Ståhlman M, Forsberg GB, Saarinen S, Nilsson R, Hansson GI. The BUME method: a novel automated chloroform-free 96-well total lipid extraction method for blood plasma. *J Lipid Res*. 2012;53:1690-1700. doi:10.1194/JLR.D023036
22. Chapman MJ, Ginsberg HN, Amarenco P, et al. Triglyceride-rich lipoproteins and high-density lipoprotein cholesterol in patients at high risk of cardiovascular disease: evidence and guidance for management. *Eur Heart J*. 2011;32:1345-1361. doi:10.1093/EURHEARTJ/EHR112
23. Cesena FY, Generoso G, Santos RD, et al. The association between triglyceride-rich lipoproteins, circulating leukocytes, and low-grade inflammation: the Brazilian longitudinal study of adult health (ELSA-brasil). *J Clin Lipidol*. 2023;17:261-271. doi:10.1016/j.jacl.2023.01.007
24. Fuertes-Martín R, Taverner D, Vallvé JC, et al. Characterization of ^{1}H-NMR plasma glycoproteins as a new strategy to identify inflammatory patterns in rheumatoid arthritis. *J Proteome Res*. 2018;17:3730-3739. doi:10.1021/acs.jproteome.8b00411
25. Malo A-I, Rull A, Girona J, et al. Glycoprotein profile assessed by ^{1}H-NMR as a global inflammation marker in patients with HIV infection. A Prospective Study. *J Clin Med*. 2020;9:1344. doi:10.3390/jcm9051344
26. Fuertes-Martín R, Moncayo S, Insenser M, et al. Glycoprotein a and B height-to-width ratios as obesity-independent novel biomarkers of low-grade chronic inflammation in women with polycystic ovary syndrome (PCOS). *J Proteome Res*. 2019;18:4038-4045. doi:10.1021/acs.jproteome.9b00528
27. Rehues P, Girona J, Guardiola M, et al. PCSK9 inhibitors have apolipoprotein C-III-related anti-inflammatory activity, assessed by ^{1}H-NMR glycoprotein profile in subjects at high or very high cardiovascular risk. *Int J Mol Sci*. 2023;24:2319. doi:10.3390/IJMS24032319/S1
28. Mokkala K, Houttu N, Koivuniemi E, Sørensen N, Nielsen HB, Laitinen K. GlycA, a novel marker for low grade inflammation, reflects gut microbiome diversity and is more accurate than high sensitive CRP in reflecting metabolomic profile. *Metabolomics*. 2020;16:76. doi:10.1007/s11306-020-01695-x
29. Kawakami A, Aikawa M, Nitta N, Yoshida M, Libby P, Sacks FM. Apolipoprotein CIII-induced THP-1 cell adhesion to endothelial cells involves pertussis toxin-sensitive G protein- and protein kinase Cα-mediated nuclear factor-κB activation. *Arterioscler Thromb Vasc Biol*. 2007;27:219-225. doi:10.1161/01.ATV.0000249620.68705.0d
30. Balling M, Afzal S, Varbo A, Langsted A, Davey Smith G, Nordestgaard BG. VLDL cholesterol accounts for one-half of the risk of myocardial infarction associated with apoB-containing lipoproteins. *J Am Coll Cardiol*. 2020;76:2725-2735. doi:10.1016/J.JACC.2020.09.610

31. Paramel Varghese G, Folkersen L, Strawbridge RJ, et al. NLRP3 inflammasome expression and activation in human atherosclerosis. *J Am Heart Assoc*. 2016;5:e003031. doi:10.1161/JAHA.115.003031/FORMAT/EPUB
32. Wang L, Gill R, Pedersen TL, Higgins LJ, Newman JW, Rutledge JC. Triglyceride-rich lipoprotein lipolysis releases neutral and oxidized FFAs that induce endothelial cell inflammation. *J Lipid Res*. 2009;50:204-213. doi:10.1194/JLR.M700505-JLR200
33. Graham VS, Lawson C, Wheeler-Jones CP, Perona JS, Ruiz-Gutierrez V, Botham KM. Triacylglycerol-rich lipoproteins derived from healthy donors fed different olive oils modulate cytokine secretion and cyclooxygenase-2 expression in macrophages: the potential role of oleanolic acid. *Eur J Nutr*. 2012;51:301-309. doi:10.1007/S00394-011-0215-2
34. Fernández-Aparicio Á, Perona JS, Castellano JM, Correa-Rodríguez M, Schmidt-Riovalle J, González-Jiménez E. Oleanolic acid-enriched olive oil alleviates the Interleukin-6 overproduction induced by postprandial triglyceride-rich lipoproteins in THP-1 macrophages. *Nutrients*. 2021;13:3471. doi:10.3390/NU13103471
35. Varbo A, Benn M, Tybjærg-Hansen A, Nordestgaard BG. Elevated remnant cholesterol causes both low-grade inflammation and ischemic heart disease, whereas elevated low-density lipoprotein cholesterol causes ischemic heart disease without inflammation. *Circulation*. 2013;128:1298-1309. doi:10.1161/CIRCULATIONAHA.113.003008/FORMAT/EPUB
36. Nicholls SJ, Lincoff AM, Garcia M, et al. Effect of high-dose Omega-3 fatty acids vs corn oil on major adverse cardiovascular events in patients at high cardiovascular risk: the STRENGTH randomized clinical trial. *JAMA*. 2020;324:2268-2280. doi:10.1001/JAMA.2020.22258
37. Das Pradhan A, Glynn RJ, Fruchart J-C, et al. Triglyceride lowering with pemafibrate to reduce cardiovascular risk. *N Engl J Med*. 2022;387:1923-1934. doi:10.1056/NEJMOA2210645/SUPPL_FILE/NEJMOA2210645_DATA-SHARING.PDF
38. Bhatt DL, Steg PG, Miller M, et al. Cardiovascular risk reduction with icosapent ethyl for hypertriglyceridemia. *N Engl J Med*. 2019;380:11-22. doi:10.1056/NEJMOA1812792

SUPPORTING INFORMATION

Additional supporting information can be found online in the Supporting Information section at the end of this article.

How to cite this article: Moreno-Vedia J, Llop D, Rodríguez-Calvo R, et al. Lipidomics of triglyceride-rich lipoproteins derived from hyperlipidemic patients on inflammation. *Eur J Clin Invest*. 2024;54:e14132. doi:10.1111/eci.14132